

## Alloying experiments on heavy fermion compounds

Frank Steglich, U. Ahlheim, C. Schank, C. Geibel, Siegfried R. Horn, M. Lang, G. Sparn, Alois Loidl, Alexander Krimmel

### Angaben zur Veröffentlichung / Publication details:

Steglich, Frank, U. Ahlheim, C. Schank, C. Geibel, Siegfried R. Horn, M. Lang, G. Sparn, Alois Loidl, and Alexander Krimmel. 1990. "Alloying experiments on heavy fermion compounds." *Journal of Magnetism and Magnetic Materials* 84 (3): 271–80.  
[https://doi.org/10.1016/0304-8853\(90\)90105-y](https://doi.org/10.1016/0304-8853(90)90105-y).

### Nutzungsbedingungen / Terms of use:

CC BY-NC-ND 4.0

## ALLOYING EXPERIMENTS ON HEAVY FERMION COMPOUNDS

F. STEGLICH, U. AHLHEIM, C. SCHANK, C. GEIBEL, S. HORN, M. LANG, G. SPARN

*Institut für Festkörperphysik, Technische Hochschule Darmstadt, D-6100 Darmstadt, Fed. Rep. Germany*

A. LOIDL and A. KRIMMEL

*Institut für Physik, Universität Mainz, D-6500 Mainz, Fed. Rep. Germany*

This paper is intended to demonstrate the usefulness of controlled alloying for the understanding of heavy-fermion physics: (1) Th-substitution for Ce in  $\text{CeCu}_2\text{Si}_2$  emphasizes the dominating role of the dopant-induced strain fields in generating incoherent scattering and pair breaking, (2) replacement of Cu by Ni in  $\text{Ce}(\text{Cu}_{1-x}\text{Ni}_x)_2\text{Ge}_2$  leads to phenomena which are interpreted as derived from a transition between local-moment and itinerant heavy-fermion magnetism, and (3) increasing Cu concentration in  $\text{UCu}_{4+x}\text{Al}_{8-x}$  is accompanied by an antiferromagnetic to nonmagnetic transition near  $x_{\text{cr}} = 1.5$  similar to what has been found before for several Ce-based systems. A heavy Fermi-liquid phase with incipient coherence of the quasiparticles is established for  $x \geq x_{\text{cr}}$ .

### 1. Characteristics of heavy-fermion compounds

Heavy-fermion compounds contain a regular lattice of f-ions, notably Ce, U and Np, whose separation is much too large for a significant f-wavefunction overlap [1]. As a consequence, local f-derived magnetic moments, weakly coupled to the Fermi sea of normal conduction electrons, are observed well above a characteristic temperature  $T^*$ , which can vary between a few and several tens kelvin. Hybridization of the local f-electron states with ligand states is essential in these systems: it causes a Kondo effect [2] at the f-ion sites, which can be inferred, e.g., from a negative temperature coefficient of the electrical resistivity  $\rho(T)$  above  $T^*$ . In addition, a gradual reduction of the slope of the magnetic susceptibility and an increase of the electronic specific heat  $\gamma T$  over that at high temperature are found when cooling the systems below  $T^*$ , the "lattice Kondo temperature". Like in the canonical dilute Kondo alloys  $\text{CuFe}$  and  $\text{LaCe}$ , the local moments become progressively screened and the magnetic (3d or 4f) electrons weakly delocalized. This is usually attributed to the formation of a sharp resonance at the Fermi energy  $E_F$ , which (in case of  $\text{Ce}^{3+}$  ions) can be visualized as a narrow band of local quasi-

particles of 4f-symmetry [3]. Since the very high density of states at  $E_F$  corresponds also to a very large effective mass of these local quasiparticles, the latter are usually called "heavy fermions" (or "heavy electrons").

In the intermetallic compounds of interest, the single-site Kondo effect competes with the magnetic intersite Rudermann-Kittel-Kasuya-Yosida (RKKY) interaction [4] which tends to restore the local magnetic moments. According to Doniach [5], the ground state of such a compound is determined by the relative strengths of the Kondo and the RKKY interactions. For the majority of the heavy-fermion compounds  $T^*$  does not exceed 10 K and is smaller than  $T_{\text{RKKY}}$ , the temperature at which short-range magnetic correlations develop. Consequently long-range magnetic order, usually of a complex antiferromagnetic type, forms below  $T_N < T_{\text{RKKY}}$ . Prototypical examples are  $\text{CeAl}_2$  [6] and  $\text{CeB}_6$  [7] with considerably reduced ordered moments and enhanced  $\gamma$  values ( $> 100 \text{ mJ/K}^2 \text{ mol f-ion}$ ) well below the Néel temperatures of 3.9 and 2.3 K, respectively.

For a limited number of compounds (with  $T^* > T_{\text{RKKY}}$ ), like, e.g.,  $\text{CeAl}_3$  [8],  $\text{CeCu}_2\text{Si}_2$  [9],  $\text{CeRu}_2\text{Si}_2$  [10],  $\text{UBe}_{13}$  [11] and  $\text{CeCu}_6$  [12], there is no evidence for the "local moment"-type long

range magnetic order. Rather a “heavy Fermi liquid” phase develops well below  $T^*$ . Specific heat coefficients  $\gamma$  of order or even in excess of  $1 \text{ J/K}^2\text{mol}$  f-ion and correspondingly enhanced Pauli-like spin susceptibilities highlight effective quasiparticle masses up to about 400 times  $m_0$ , the free-electron mass [1]. In contrast to dilute Kondo alloys which show maximum electrical resistivity at  $T \rightarrow 0$ , a peak in the f-increment of  $\rho(T)$  occurs at a finite temperature  $T_p \approx T^*$  [1]. Very small resistivity values are found at low temperatures. The  $T$ -dependence,  $\rho = \rho_0 + AT^2$  ( $\rho_0$ : residual resistivity), indicates dominating electron–electron scattering. Since the coefficient  $A$  ( $\sim m^{*2}$ ) exceeds the corresponding values for simple metals by several orders of magnitude, itinerant heavy fermion states are involved in this process. The resistivity results beautifully demonstrate Bloch’s theorem according to which a perfect lattice of f-ions (“Kondo lattice”) should give rise to extended (“Bloch”) states [13]. De Haas–van Alphen experiments have proven that coherent, i.e., itinerant, heavy fermions in fact exist at very low temperatures in both  $\text{CeCu}_6$  [14] and  $\text{UPt}_3$  [15].

Though very interesting in itself, most of the excitement about the low- $T$  heavy Fermi liquid phase in the Kondo lattice originated from its instability against superconducting and magnetic phase transitions. Four heavy fermion superconductors,  $\text{CeCu}_2\text{Si}_2$  [9],  $\text{UBe}_{13}$  [11],  $\text{UPt}_3$  [16] and  $\text{URu}_2\text{Si}_2$  [17] are known. From gigantic absolute values at  $T_c$  of both the height of the specific-heat jump and the slope of the upper critical field, the Cooper pairs appear to be formed by heavy fermions. Non-exponential temperature dependencies of the specific heat and related transport coefficients hint at strongly anisotropic order parameters [1]. Simple power-law dependencies in these quantities and complex phase diagrams containing more than one superconducting phase like in  $\text{UPt}_3$  [18] are often interpreted as derived from exotic, i.e., non-phononic, pairing mechanisms. In particular, magnetic couplings seem to play an important role, mainly because heavy fermion superconductivity is found close to a new kind of “band-like” magnetism, characterized by extremely small ordered moments ( $\approx 10^{-2}\mu_B/\text{f-ion}$ ):

a spin-density wave (SDW) transition at  $T_N = 17 \text{ K}$  was discovered [17] for  $\text{URu}_2\text{Si}_2$  to be followed by a superconducting one at  $T_c = 1.5 \text{ K}$ . A similar situation seems to exist in the low- $T$  phase of  $\text{UPt}_3$  [19]. Specific-heat experiments suggest the occurrence of antiferromagnetism in  $\text{UBe}_{13}$  below  $0.15 \text{ K}$  and for magnetic fields  $B \geq 2 \text{ T}$  ( $T_c \approx 0.9 \text{ K}$ ) [20]. For  $\text{CeCu}_2\text{Si}_2$ ,  $\mu\text{SR}$  results at  $B = 0 \text{ T}$  are consistent with the onset of long range antiferromagnetism at  $T_N \approx 0.8 \text{ K}$  [21], whereas NMR [22] and magnetoresistivity [23] anomalies have led to the assumption of a low- $T$  phase diagram with superconductivity below  $B_{c2}(0) \approx 2 \text{ T}$  [24], (itinerant) antiferromagnetism up to  $B \approx 7 \text{ T}$  and coexistence of the two between 1 and 2 T [25].

Whereas presently no conclusive pictures are at hand concerning the microscopic nature of heavy fermion superconductivity and heavy fermion band magnetism it has become clear that these phenomena are as sensitive to impurities as the coherent Fermi liquid phase itself. Controlled alloying is, therefore, considered a suitable means of probing specific properties of the different ground states. As an example, we shall discuss in the subsequent section recent investigations on Ce substitution in normal-state and superconducting  $\text{CeCu}_2\text{Si}_2$ , which emphasize the destructive effect of impurity-induced strain fields [26].

In the past alloying was very successfully used to induce transitions between different ground states, e.g., from either superconductivity [27] or a

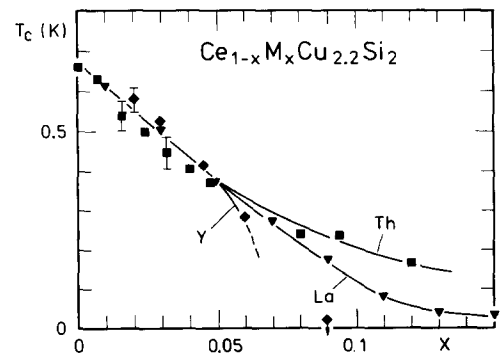


Fig. 1. Transition temperature  $T_c$  vs. concentration  $x$  of  $\text{Ce}_{1-x}\text{M}_x\text{Cu}_{2.2}\text{Si}_2$  with  $M = \text{Y}$  (◆),  $M = \text{La}$  (▼) and  $M = \text{Th}$  (■). Lines drawn are guides to the eye.

Fermi liquid [28] to antiferromagnetism. In this paper, we shall focus on quasibinary alloy systems retaining the periodicity of the f-ion lattice. For the first time it appears to be possible to monitor a transition between local-moment and itinerant heavy fermion magnetism in  $\text{Ce}(\text{Cu}_{1-x}\text{Ni}_x)_2\text{Ge}_2$  [29] (section 3). In addition, a transition between a magnetically ordered and a heavy Fermi liquid ground state in  $\text{UCu}_{4+x}\text{Al}_{8-x}$  has recently been established [30], which will be the subject of section 4.

## 2. Impurity effects on coherence and superconductivity: $\text{Ce}_{1-x}\text{Th}_x\text{Cu}_2\text{Si}_2$

Non-magnetic dopants substituting f-ions in a Kondo lattice, often termed “Kondo holes”, can seriously affect normal (n)-state and superconducting properties. For example, the low- $T$  peak in the resistivity is usually shifted downwards, indicating an increase in incoherent scattering at low temperature, which goes along with an efficient depression of the superconducting transition temperature [31–33]. The observation that the specific heat jump height  $\Delta C$  at the transition is depressed even stronger than  $T_c$  reflects an increase in the density of states (DOS) at low excitation energies [33]. For an illustration, the effect of La and Y doping in  $\text{CeCu}_{2.2}\text{Si}_2$  on  $T_c$  and  $\Delta C^* = \Delta C/\gamma(T_c)$ , where  $\gamma(T_c) = C_n(T_c)/T_c$ , is shown in figs. 1 and 2. These results resemble the pair-breaking effect by magnetic dopants in a BCS superconductor [34] and have, therefore, been ascribed to a “pair-breaking” by non-magnetic impurities in heavy fermion superconductors [35]. In contrast to the former case, where breaking of time-reversal symmetry by the impurity spin leads to a partial filling of the gap, it is believed that smearing of anisotropies in the orbital part of the Cooper-pair wavefunction is essential in the latter case. This has been labelled a “diamagnetic pair breaking by impurities” [35]. An additional paramagnetic pair breaking by the 4f spin, acting on the spin state of the Cooper pairs, was inferred from results on Gd- and Pr-doped  $\text{CeCu}_{2.2}\text{Si}_2$  samples [35].

According to figs. 1 and 2, Y dopants are more

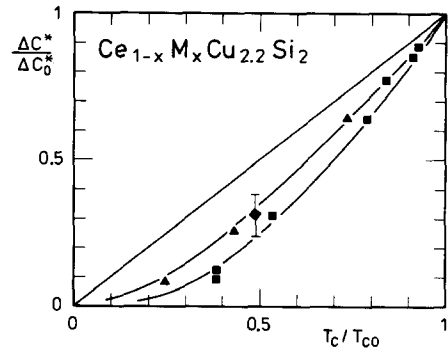


Fig. 2. Reduced specific heat jump,  $\Delta C^*/\Delta C_0^* = \gamma^{-1}(x, T_c)\Delta C(x)/\gamma^{-1}(0, T_c)\Delta C(0)$  vs reduced transition temperature,  $T_c(x)/T_c(0)$ , for  $\text{Ce}_{1-x}\text{M}_x\text{Cu}_{2.2}\text{Si}_2$  with  $M = \text{Y}$  ( $\blacklozenge$ ),  $M = \text{La}$  ( $\nabla$ ) and  $M = \text{Th}$  ( $\blacksquare$ ). The diagonal line shows the result for the BCS-theory (“law of corresponding states”), the other lines are guides to the eye. For the point of the thoriated sample, an error bar is drawn.

efficient pair breakers than La dopants, which correlates with a larger incoherent scattering in the normal state induced by the former [33]. As possible sources for these different scattering potentials the differences, in either the electronic structure or the ionic size relative to Ce have been discussed [33]. In both respects, Y deviates more strongly from Ce than La: its valence-electron configuration is  $4d^15s^2$  rather than  $5d^16s^2$  (as for both La and Ce), and its size mismatch to Ce exceeds that of La. In order to minimize the size mismatch, i.e., the strain fields around the dopants, Th impurities have been substituted for Ce in  $\text{CeCu}_{2.2}\text{Si}_2$ . Since their valence-electron configuration ( $6d^77s^2$ ) differs from that of Ce, results on Th-doped samples should help to decide which of the two afore-mentioned properties of the dopants dominates in affecting the coherent Fermi-liquid phase and the superconducting phase.

Specific-heat results on several polycrystalline samples with  $0 \leq x \leq 0.12$  are shown in fig. 3a for zero magnetic field and in fig. 3b for  $B = 2$  T. We first address the n-state properties. The broad maximum in  $C_n(T)/T = \gamma(T)$  at  $T_0 \approx 0.45$  K, which is found for undoped  $\text{CeCu}_{2.2}\text{Si}_2$ , has been ascribed to the interference of the coherent 4f (heavy fermion) band, which forms at low  $T$  near  $E_F$ , with ordinary conduction bands [36]. Doping with less than 3 at% of either La or Y was found

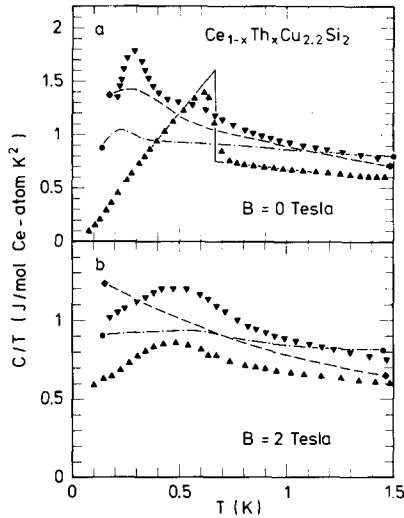


Fig. 3. Specific-heat results for several  $\text{Ce}_{1-x}\text{Th}_x\text{Cu}_{2.2}\text{Si}_2$  alloys in a  $C/T$  vs  $T$  plot. Concentrations are  $x = 0$  (▲),  $x = 0.03$  (■),  $x = 0.055$  (▼),  $x = 0.08$  (◆ and dashed line) and  $x = 0.12$  (● and dash-dotted line). The construction of an idealized jump is sketched for the case  $x = 0$ . (a) shows the data at  $B = 0$  T, in (b) an overcritical field of  $B = 2$  T was applied.

to remove this structure, leaving behind a very flat maximum similar to the one displayed for the 12 at% Th sample in fig. 3b. No significant change in  $\gamma(T)$ , however, is found for Th concentrations up to 5.5 at%. (The increase of  $\gamma(T)$  at a fixed temperature may reflect an increasing valence-excitation energy: Th is tetravalent and supplies an additional electron to the conduction band which shifts the Fermi energy upwards, thus stabilizing the magnetic  $\text{Ce}^{3+}$  configuration.) The relative insensitivity of the coherent Fermi liquid phase of  $\text{CeCu}_{2.2}\text{Si}_2$  against Th (compared to La and Y) doping supports the dominance of the size mismatch rather than the valence-electron configuration of the Kondo holes [26] as a major source for incoherent scattering and pair breaking [31–33].

The strong Th-induced depression of the specific heat jump height confirms the “diamagnetic pair breaking” earlier concluded for La and Y doped samples (fig. 2).

The initial drop of the transition temperature due to Th dopants is very similar to the La- and Y-induced  $T_c$  depression (fig. 1). However, for  $x > 5$  at%, systematic differences are stated:

whereas  $T_c(x)$  exhibits a positive curvature and a critical concentration (as  $T_c \rightarrow 0$ )  $x_{\text{cr}} < 9$  at% for  $M = \text{Y}$ , a negative curvature of  $T_c(x)$  is found for both  $M = \text{La}$  and  $\text{Th}$ . The critical concentrations are  $x_{\text{cr}} \leq 15$  at% for La and  $x_{\text{cr}} \approx 20$  at% for Th dopants, respectively. To summarize, Th impurities substituted for Ce appear to be less harmful to heavy-fermion superconductivity in  $\text{CeCu}_{2.2}\text{Si}_2$  than La and Y impurities. A similar observation was reported for Th dopants substituting U in  $\text{UBe}_{13}$  [32]. However, no indication for a second superconducting transition like the one in  $\text{U}_{1-x}\text{Th}_x\text{Be}_{13}$  [37,38] has been resolved in  $\text{Ce}_{1-x}\text{Th}_x\text{Cu}_{2.2}\text{Si}_2$ .

### 3. Transition from local-moment to band magnetism: $\text{Ce}(\text{Cu}_{1-x}\text{Ni}_x)_2\text{Ge}_2$

Whereas a number of examples are known for both local-moment ordering like in  $\text{CeAl}_2$  [6] and “band magnetism” like in  $\text{UPt}_3$  [19], a transition between the two phenomena (by either applying external pressure or alloying) has not been observed until recently. Such an investigation, starting from a suitable local-moment antiferromagnet with  $T^* \approx T_{\text{RKKY}}$  should leave the f-ion lattice undisturbed. In the following, results on quasibinary  $\text{Ce}(\text{Cu}_{1-x}\text{Ni}_x)_2\text{Ge}_2$  alloys are presented that are compatible with a transition between the two different kinds of cooperative magnetism [29].

The compound  $\text{CeCu}_2\text{Ge}_2$ , which crystallizes in the tetragonal  $\text{ThCr}_2\text{Si}_2$  structure (lattice parameters  $a = 4.17$  Å and  $c = 10.20$  Å), appeared as an ideal system to start with: its Kondo-binding energy  $k_B T^*$  ( $T^* \approx 6$ –8 K [39]) is of the same magnitude as the magnetic interaction energy, since short range ordering was inferred to set in at  $T_{\text{RKKY}} \approx 7$  K [39]. Long range antiferromagnetic order has been discovered by several techniques [40,39] below  $T_N = 4.1$  K. The magnetic structure of  $\text{CeCu}_2\text{Ge}_2$  is incommensurate with the chemical cell (see below), and the ordered moment  $\mu_s$  at  $T = 1.5$  K amounts to  $0.74\mu_B/\text{Ce}$ . This is smaller by a factor of two compared to  $\mu_s$  expected from the crystal field (CF) ground state doublet, which has been determined by inelastic neutron scattering experiments [39]. Because  $T^* \approx T_{\text{RKKY}}$ , the

reduction of the Ce moment is ascribed to the Kondo effect. It is related to the observation of quasi-elastic magnetic neutron scattering intensity which is observed in the antiferromagnetic state, in addition to inelastic spin-wave derived scattering intensity [5]. In addition, a strongly enhanced electronic specific heat  $C_e(T) = \gamma(T) \cdot T$  was discovered well below  $T_N$ , i.e., in the presence of magnon-derived and nuclear contributions. The temperature dependence of  $\gamma(T)$  exhibits a maximum at 0.45 K and, thus, strongly resembles  $\gamma(T)$  as established for prototypical heavy-fermion compounds like  $\text{CeAl}_3$  and normal-state  $\text{CeCu}_2\text{Si}_2$  [36].  $\text{CeNi}_2\text{Ge}_2$  is isostructural to  $\text{CeCu}_2\text{Ge}_2$  with somewhat reduced lattice parameters ( $a = 4.15 \text{ \AA}$ ,  $c = 9.84 \text{ \AA}$ ). No magnetism could be detected for this material, which rather exhibits the signatures of a Kondo lattice, such as a maximum in the Sommerfeld coefficient  $\gamma(T)$  at 0.3 K. Both  $\gamma_{\text{max}} \approx 0.4 \text{ J/K}^2 \text{ mol}$  and  $T^* \approx 30 \text{ K}$  characterize  $\text{CeNi}_2\text{Ge}_2$  as a heavy-fermion compound, for which no indications of CF excitations could be found up to now [41].

Figure 4a shows the concentration dependence of the characteristic temperature  $T^*$  for

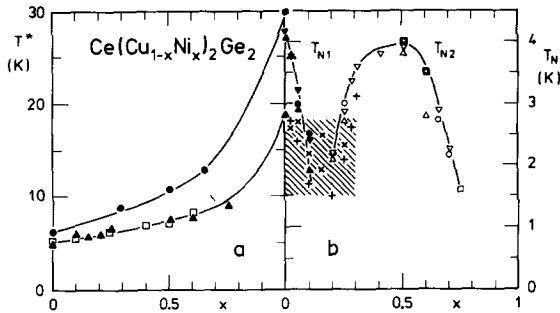


Fig. 4. (a) Characteristic temperature  $T^*$  read off positions of broad thermal-expansion  $\alpha(T)$  peaks ( $\square$ ), resistivity  $\rho(T)$  peaks ( $\blacktriangle$ ) as well as residual quasi-elastic line widths (HWHM)  $\Gamma(0)$  extrapolated from  $T > 50 \text{ K}$  to  $T = 0 \text{ K}$  ( $\bullet$ ). In order to match  $\alpha(T)$  and  $\rho(T)$  results,  $\rho(T)$  peak positions are scaled by a factor 1.25. (b) Positions of extrema, indicating antiferromagnetic phase transitions, in  $\alpha(T)$  ( $\blacktriangle$ ,  $\triangle$ ,  $\times$ ), specific heat  $C(T)$  ( $\blacktriangledown$ ,  $\triangledown$ ,  $+$ ),  $\rho(T)$  ( $\square$ ) and dc-susceptibility ( $\bullet$ ,  $\circ$ ). Closed symbols refer to onset of "local-moment ordering" below  $T_{N_1}(x)$ , open symbols indicate formation of "itinerant magnetism" below  $T_{N_2}(x)$ , crosses are ascribed to superposition of two modulated structures at intermediate composition (hatched), see text.

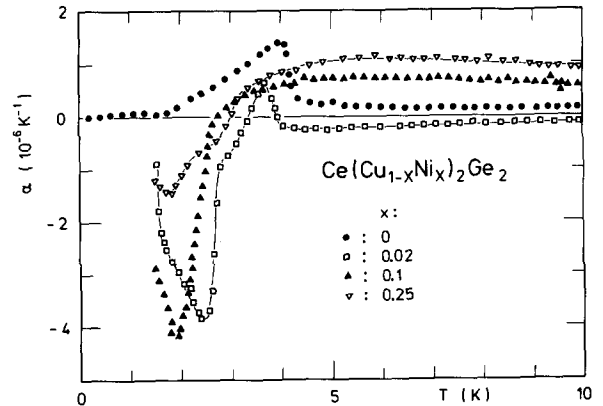


Fig. 5.  $\alpha$  vs  $T$  for several  $\text{Ce}(\text{Cu}_{1-x}\text{Ni}_x)_2\text{Ge}_2$  alloys. Solid lines are guides to the eye.

$\text{Ce}(\text{Cu}_{1-x}\text{Ni}_x)_2\text{Ge}_2$ , as determined by the residual value of the quasi-elastic neutron scattering line width (HWHM)  $\Gamma(0)$ , extrapolated linearly from  $T > 50 \text{ K}$  to  $T = 0$ .  $T^*(x)$  is tracked by the positions of broad maxima in the coefficient of thermal expansion  $\alpha(T)$  (fig. 5), and by low- $T$   $\rho(T)$  peaks which, in accord with theoretical expectations [43], occur at somewhat lower temperatures.  $T^*$  increases steadily as a function of Ni concentration so that, finally, the binding energy for the Kondo-singlet state exceeds the gain in energy due to the formation of magnetic order. Interestingly enough, cooperative magnetism disappears near  $x = 0.75$ , where  $T^*(x)$  shows a distinct increase in slope, associated with the disappearance of CF-splitting derived anomalies. Figure 4b shows the concentration dependence of the Néel temperature,  $T_N(x)$ , as determined from  $\alpha(T)$  (fig. 5) and  $C(T)$  (fig. 6) measurements: already a marginal substitution of Ni for Cu in  $\text{CeCu}_2\text{Ge}_2$  causes a rapid drop of the Néel temperature  $T_{N_1}(x)$ , which extrapolates to zero near 20 at% Ni. However, a second branch,  $T_{N_2}(x)$ , develops for  $x > 0.2$ . It assumes a maximum of  $\approx 4 \text{ K}$  near  $x = 0.5$  and can be monitored up to  $x = 0.75$ . Different kinds of magnetic ordering below  $T_{N_1}$  and  $T_{N_2}$  have already been inferred in ref. [42] from different signs in the jump-like  $\alpha(T)$  anomalies associated with these phase transitions, cf. fig. 5.

In addition to these preliminary results [42], we have observed double-peak structures in  $\alpha(T)$  and

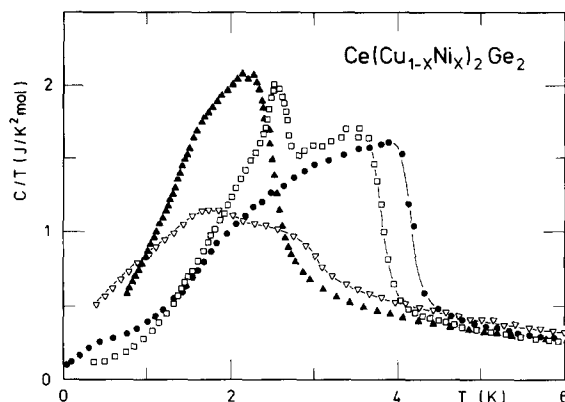


Fig. 6.  $C/T$  vs.  $T$  for same  $\text{Ce}(\text{Cu}_{1-x}\text{Ni}_x)_2\text{Ge}_2$  alloys (indicated by same symbols as in fig. 2). Solid lines are guides to the eye.

$C(T)$  for concentrations  $0.02 \leq x \leq 0.3$ . Already 2 at% Ni substitution causes pronounced anomalies below the Néel temperature  $T_{N1} = 3.8$  K, i.e., a sharp peak in  $C(T)$  (fig. 6) and a large negative jump in  $\alpha(T)$  which contrasts to the positive one at  $T_{N1}$  (fig. 5). While the two anomalies nearly merge and therefore cannot easily be separated in the intermediate concentration range  $0.1 \leq x \leq 0.2$ , the data points for the 25 at% Ni system again reveal two distinguishable maxima, which for  $\alpha(T)$  both appear to be of negative sign (fig. 5). The additional low- $T$  anomalies track the concentration dependencies of the respective  $T_{N1}(x)$  and  $T_{N2}(x)$  values.

In order to determine the magnetic structures and the size of the ordered moments in these materials, neutron powder-diffraction experiments have been performed. The powder diffraction spectra previously obtained for  $\text{CeCu}_2\text{Ge}_2$  [39] are reproduced in fig. 7a and compared with the corresponding spectra for  $\text{Ce}(\text{Cu}_{1-x}\text{Ni}_x)_2\text{Ge}_2$  alloys with  $x = 0.1, 0.28$  and  $0.5$  (fig. 7b-d). In all cases, the intensities as measured in the paramagnetic phase (at  $T = 6$  K) were subtracted from the spectra as measured in the magnetically ordered phase at 1.5 K. All the systems studied exhibit a magnetic structure incommensurate with the chemical lattice. The positions of the magnetic reflections can be indexed in terms of  $\mathbf{Q} = \tau_{\text{hkl}} \pm \mathbf{q}_0$ , where  $\tau_{\text{hkl}}$  is a vector of the nuclear reciprocal lattice and  $\mathbf{q}_0$  is the propagation vector of a modulated spin

arrangement. In  $\text{CeCu}_2\text{Ge}_2$  the best fit to the observed magnetic intensities was obtained by choosing a single-plane spiral, with the phase of rotation perpendicular to the propagation vector (whose components are given in units of  $2\pi/a$ ,  $2\pi/a$  and  $2\pi/c$ ),  $\mathbf{q}_0 = (0.28, 0.28, 0.54)$ . The results for the 10 at% Ni sample shown in fig. 7b look very similar, although the modulation vector is slightly changed to  $\mathbf{q}_0 = (0.28, 0.28, 0.41)$ . Dramatic changes of the diffraction patterns occur, however, for  $x = 0.28$  (fig. 7c) and  $x = 0.5$  (fig. 7d). The Bragg angles of the magnetic reflections for  $x = 0.5$  can be indexed assuming that the two dominating lines are satellites of the nuclear (002) reflection. This yields a propagation vector  $\mathbf{q}_0 = (0, 0, 0.13)$ . Future work on single crystals will be necessary to check this assignment. Such experiments are also required to reveal the  $x$  dependence of the ordered moment  $\mu_s$ . The present powder diffraction data suggest a gradual decrease of  $\mu_s(x)$ , reaching a value of the order of  $\approx 0.5 \mu_B/\text{Ce}$  for  $x = 0.5$ . For  $x = 0.65$ , no long range magnetic order can be resolved by neutron diffraction, in contrast to the  $\alpha(T)$  and  $C(T)$  measurements which reveal clear-cut phase transition anomalies (fig. 4b). Therefore,  $\mu_s$  is estimated to be smaller than  $0.2 \mu_B/\text{Ce}$  for  $x \geq 0.65$ .

Our neutron-diffraction results support the conclusion derived from bulk measurements that two different kinds of antiferromagnetic order ex-

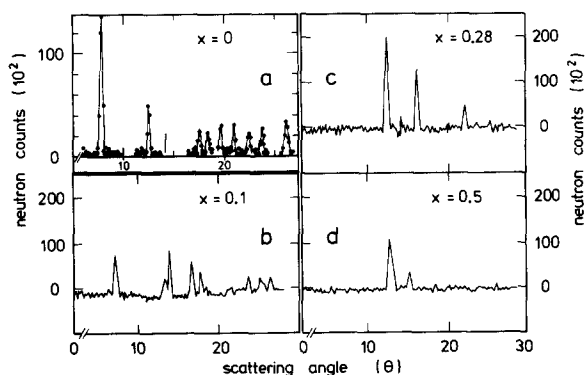


Fig. 7. Neutron powder-diffraction patterns, scattering intensity vs. scattering angle, for  $\text{CeCu}_2\text{Ge}_2$  (a) and  $\text{Ce}(\text{Cu}_{1-x}\text{Ni}_x)_2\text{Ge}_2$  with different  $x$  (b-d). Difference spectra ( $I(1.5 \text{ K}) - I(6 \text{ K})$ ) are shown to display magnetic satellites to nuclear Bragg reflections only.

ist below  $T_{N_1}(x)$  and  $T_{N_2}(x)$ . Since both magnetic structures are incommensurate with the lattice, with modulation vectors  $q_{01}$  and  $q_{02}$ , a superposition of them may cause a further increase of the magnetic condensation energy [29]. Taking into account the existence of double-phase transitions in the concentration range  $0.02 \leq x \leq 0.3$ , we propose as a working hypothesis for future studies: (1) the upper of these two transitions indicates the formation of a modulated magnetic structure characterized either by  $q_{01}$  if  $x < 0.15$ , or by  $q_{02}$  for  $x > 0.15$  (cf. fig. 4b), and (2) at the lower transition, this structure becomes superposed by that one with the alternate  $q_0$  vector, so that actually a state characterized by  $q_{01} \pm q_{02}$  is formed at sufficiently low  $T$ . In fact, a superposition of the  $q_0$  vectors determined for  $x = 0$  and  $x = 0.5$  results in  $q_0 = (0.28, 0.28, 0.41)$  as measured for the system with intermediate concentration,  $x = 0.1$ .

The occurrence of extremely short propagation vectors which characterize a modulated spin arrangement extending over almost ten lattice

constants appears very puzzling at first glance. However, in a perturbational approach to the Anderson lattice using an idealized hybridized band structure. Grewe and Welslau [44] predicted that "band magnetism", developing out of the heavy Fermi liquid phase of a Kondo-lattice system, should involve  $q_0$  vectors as short as the one derived from our powder spectra. Based on the available data we preliminary suggest the following two-band picture: in the  $\text{CeCu}_2\text{Ge}_2$  compound (as well as in the  $\text{CeM}_2\text{Ge}_2$ ,  $M = \text{Ag, Au}$  homologs [45]) coherent Fermi liquid effects in the specific heat coexist with local-moment ordering, presumably on different parts of the Fermi surface. Already small Ni substitution (2 at %) leads to the disappearance of the "coherence peak" in  $\gamma(T)$  and to the development of the small- $q_0$  ordering, which seems to be superposed with the large- $q_0$  modulation forming below  $T_{N_1} = 3.8$  K (fig. 6). The strong "initial" increase in  $T_{N_2}(x)$ , when  $x$  is increased from 0.2 to 0.5, may reflect an increasing portion of the Fermi surface involved in the itinerant magnetic phase. Finally, for  $x > x_m =$

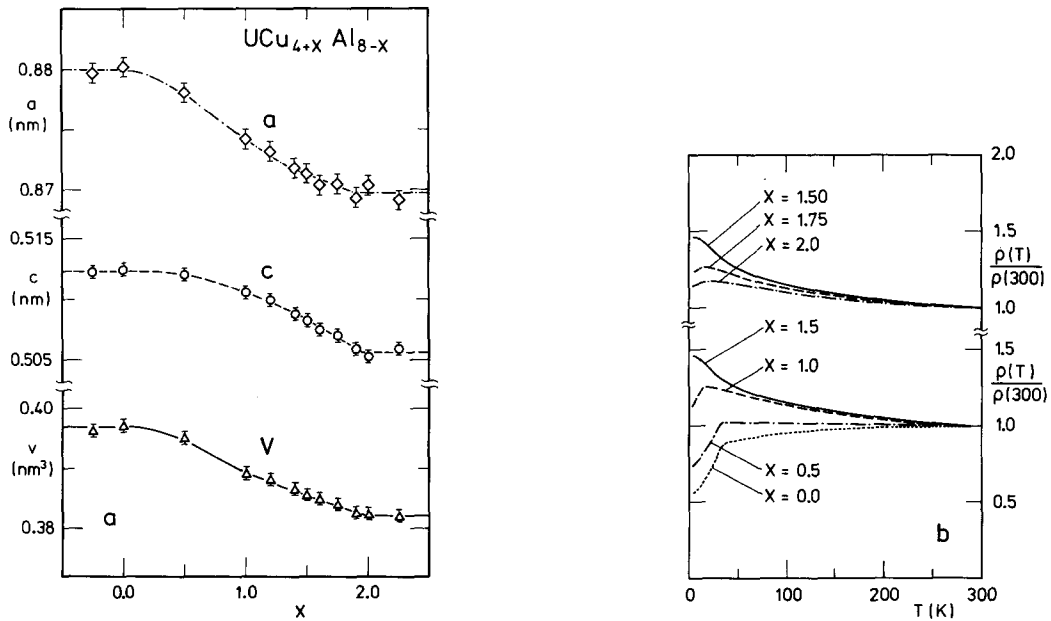


Fig. 8. (a) Lattice constants  $a$  and  $c$  and volume  $V$  of the unit cell in  $\text{UCu}_{4+x}\text{Al}_{8-x}$  as a function of  $x$ . Lines are guides to the eye. (b) Temperature dependence of the electrical resistivity between 4.2 and 300 K for different single phase  $\text{UCu}_{4+x}\text{Al}_{8-x}$  compounds. The resistivity is scaled to its value at 300 K.



0.75 no magnetic order exists owing to the Kondo interaction, which now dominates over any kind of magnetic interactions.

#### 4. Search for new systems: $\text{UCu}_{4+x}\text{Al}_{8-x}$

In this section we shall in part describe a recent investigation [30] of the ternary phase diagram of the U–Cu–Al system. Concentrating on the region with less than 20 at% U, one has so far identified three intermetallic compounds, i.e.,  $\text{U}_2\text{Cu}_7\text{Al}_3$  [46],  $\text{UCu}_4\text{Al}_8$  and  $\text{U}_2\text{Cu}_7\text{Al}_{10}$  [47,48]. In the preliminary investigations  $\text{UCu}_4\text{Al}_8$ , which crystallizes in the  $\text{ThMn}_{12}$ -structure, revealed antiferromagnetic ordering below 30 K [49] and a substantially enhanced  $\gamma$  of  $\approx 100 \text{ mJ/K}^2 \text{ mol}$  [50]. The new results show that  $\text{UCu}_{4+x}\text{Al}_{8-x}$  has a wide homogeneity range ( $0.1 \leq x \leq 1.95$ ), and that replacement of Al by Cu induces a transition from a magnetically ordered to a non-magnetic heavy fermion ground state.

The evolution of lattice parameters and cell volume as a function of composition in  $\text{UCu}_{4+x}\text{Al}_{8-x}$  is shown in fig. 8a. From the amount of impurity phase present in samples with  $x \leq 0$  and  $x \geq 2.0$ , it was concluded that the homogeneity range extends from  $x = 0.1$  to  $x = 1.95$  [30]. When Al is replaced by Cu, the  $a$  and  $c$  lattice parameters decrease and, thus, also the unit-cell volume in accordance with the difference in atomic radii (Cu: 1.28 Å; Al: 1.43 Å). It seems that the excess Cu is distributed at random on the inequivalent Al sites of the  $\text{ThMn}_{12}$  structure.

The overall physical behavior is depicted by the thermal variation of the electrical resistivity  $\rho(T)$  for different compositions (fig. 8b). For  $x = 0$ ,  $\rho$  is almost constant between 45 and 300 K. At  $T_N = 42 \text{ K}$ , the transition into the antiferromagnetic state leads to a pronounced drop in  $\rho(T)$ . With increasing Cu content, the transition shifts to lower temperature and disappears for  $x > 1.0$ . While  $T_N$  is decreasing, a Kondo-like  $\rho(T)$  dependence develops in the paramagnetic regime, which is most pronounced for  $\text{UCu}_{5.5}\text{Al}_{6.5}$ . At this composition, a maximum of the resistivity forms at  $\sim 6 \text{ K}$ . Further increase of the Cu content depresses the Kondo-like  $\rho(T)$  dependence and shifts the maxi-

mum towards higher temperatures. The reduction in  $T_N$  upon increasing  $x$  is well reflected by the  $T$ -dependence of the magnetic susceptibility  $\chi(T)$ . Above 100 K  $\chi(T)$  approximately follows a Curie–Weiss behavior, the effective moment varying between  $2.60\mu_B$  for  $x = 0.5$  and  $2.80\mu_B$  for  $x = 1.5$ . Measurements of the specific heat between 0.3 and 9 K show that the Sommerfeld coefficient  $\gamma(T \rightarrow 0)$  increases with increasing Cu content from  $\approx 100 \text{ mJ/K}^2 \text{ mol}$  for the magnetically ordered system  $\text{UCu}_5\text{Al}_7$  to about  $800 \text{ mJ/K}^2 \text{ mol}$  for the non-magnetic compound  $\text{UCu}_{5.75}\text{Al}_{6.25}$  [51].

In conclusion, increasing substitution of Cu for Al in  $\text{UCu}_{4+x}\text{Al}_{8-x}$  results in a transition from a magnetically ordered to a non-magnetic heavy fermion ground state. This transition is characterized by a linear decrease of the Néel temperature, which extrapolates to  $T = 0$  for  $x \leq 1.5$ , and the appearance of Kondo-like behavior in the resistivity. A broad maximum in  $\rho(T)$  indicates that coherent scattering from the periodic U-sublattice starts to develop even in the presence of a large residual resistivity which appears to be unavoidable in view of the random Cu–Al distribution.

Our results lead to the following picture: the 5f electrons in  $\text{UCu}_{4+x}\text{Al}_{8-x}$  behave as localized electrons owing to the low U concentration and the large U–U separation. Increasing Cu concentration causes a volume compression, i.e., an enhanced 5f-ligand hybridization. In the spirit of Doniach's phase diagram [5], the 5f-conduction electron exchange coupling constant  $|J|$  is raised from below to above  $|J_c|$ , where  $|J_c|$  is the critical value at which antiferromagnetic order disappears. The ternary system  $\text{UCu}_{4+x}\text{Al}_{8-x}$  constitutes an illuminating example for the formation of a Kondo-lattice or heavy fermion phase out of an antiferromagnetically ordered phase via changes in the chemical composition. This case is especially rare for actinide-based systems.

#### 5. Summary

The value of alloying experiments for unraveling the physics of heavy fermion compounds has

been demonstrated through three case studies: (2) By comparing results for different "Kondo holes" in  $\text{CeCu}_2\text{Si}_2$ , i.e., non-magnetic impurities on Ce-sites, the relevance of the size mismatch between Ce and the respective dopant could be demonstrated; the strength of both impurity-induced incoherent scattering and pair breaking appears to be predominated by the amplitude of the strain fields generated by the substitutional disorder in the f-ion sublattice, rather than by the difference in valence-electron concentration between Ce and the respective dopants. (2) Alloying-induced changes of the conduction band density of states at  $E_F$  and of the atomic volume cause dramatic changes in the ground state properties of  $\text{Ce}(\text{Cu}_{1-x}\text{Ni}_x)_2\text{Ge}_2$ . Successively, local-moment ordering ( $x < 0.2$ ), heavy fermion band magnetism ( $0.2 < x \leq 0.75$ ) and heavy Fermi liquid behavior ( $x > 0.75$ ) could be identified in this quasibinary system with periodic Ce sublattice. (3) Replacement of Al by Cu in the compound  $\text{UCu}_{4+x}\text{Al}_{8-x}$  leads, for  $x \geq 1.5$ , to a suppression of antiferromagnetism, presumably of the local-moment type, and to the formation of a Kondo-lattice phase, characterized by the presence of heavy fermions ( $\gamma(T \rightarrow 0) \approx 0.8 \text{ J/K}^2 \text{ mol}$  for  $x = 1.75$ ) which are on the verge of becoming itinerant as inferred from the occurrence of a low- $T$  maximum in the electrical resistivity. Because of the large U-U separation and the localized nature of the 5f electrons,  $\text{UCu}_{4+x}\text{Al}_{8-x}$  is a promising actinide system for the study of magnetic to non-magnetic transitions as in  $\text{Ce}(\text{Cu}_{1-x}\text{Ni}_x)_2\text{Ge}_2$ .

## Acknowledgements

The authors are grateful for pertinent discussions with and very helpful comments from A.L. Giorgi, N. Grewe, K. Knorr and M. Tachiki. This work was supported by the Deutsche Forschungsgemeinschaft under the auspices of the Sonderforschungsbereich 252 Darmstadt/Frankfurt/Mainz.

## References

- [1] For review articles, see; G.R. Stewart, *Rev. Mod. Phys.* 56 (1984) 755.  
F. Steglich, *Springer Series in Solid-State Sciences* 62 (1985) 23.  
C.M. Varma, *Comments on Solid State Phys.* 11 (1985) 221.  
P.A. Lee, T.M. Rice, J.W. Serene, J.L. Sham and J.W. Wilkins, *Comments Cond. Mat. Phys.* 12 (1986) 99.  
H.R. Ott, *Progr. Low Temp. Phys.* XI (1987) 217.  
P. Fulde, J. Keller and G. Zwirnagl, *Solid State Phys.* 41 (1988) 1.  
N. Grewe and F. Steglich, in: *Handbook on the Physics and Chemistry of Rare Earths*, vol. 14, eds. K.A. Gschneidner, Jr. and L. Eyring (North-Holland, Amsterdam, 1990) forthcoming.
- [2] For a review, see: J. Kondo, *Solid State Phys.* 23 (1969) 183.
- [3] See, e.g., G. Grüner and A. Zawadowski, *Rep. Progr. Phys.* 37 (1974) 1497.
- [4] M.A. Ruderman and C. Kittel, *Phys. Rev.* 96 (1954) 99.  
T. Kasuya, *Progr. Theor. Phys.* (1956) 45.  
K. Yosida, *Phys. Rev.* 106 (1957) 895.
- [5] S. Doniach, *Physica B* 91 (1977) 231.
- [6] B. Barbara, J.X. Boucherle, J.L. Buevoz, M.F. Rossignol and J. Schweizer, *Solid State Commun.* 24 (1977) 481.  
C.D. Bredl, F. Steglich and K.D. Schotte, *Z. Phys. B* 29 (1978) 327.
- [7] K. Winzer and W. Felsch, *J. de Phys.* 39 (1978) C6-832.  
M. Kawakami, S. Kunii, T. Komatsubara and T. Kasuya, *Solid State Commun.* 36 (1980) 435.
- [8] K. Andres, J.E. Graebner and H.R. Ott, *Phys. Rev. Lett.* 35 (1975) 1779.
- [9] F. Steglich, J. Aarts, C.D. Bredl, W. Lieke, D. Meschede, W. Franz and H. Schäfer, *Phys. Rev. Lett.* 43 (1979) 1892.
- [10] L.C. Gupta, D.E. MacLaughlin, Cheng Tien, C. Godart, M.A. Edwards and R.D. Parks, *Phys. Rev. B* 28 (1983) 3678.
- [11] H.R. Ott, H. Rudigier, Z. Fisk and J.L. Smith, *Phys. Rev. Lett.* 50 (1983) 1595.
- [12] Y. Onuki, Y. Shimizu and T. Komatsubara, *J. Phys. Soc. Jpn.* 53 (1984) 1210.  
G.R. Stewart, Z. Fisk and M.S. Wire, *Phys. Rev. B* 30 (1984) 482.
- [13] N.F. Mott, *Phil. Mag.* 30 (1974) 403.
- [14] P.H. Reinders, M. Springford, P.T. Coleridge, R. Boulet and D. Ravot, *Phys. Rev. Lett.* 57 (1986) 1631.
- [15] L. Taillefer, R. Newbury, G.G. Lonzarich, Z. Fisk and J.L. Smith, *J. Magn. Magn. Mat.* 63 & 64 (1987) 372.  
L. Taillefer and G.G. Lonzarich, *Phys. Rev. Lett.* 60 (1988) 1570.
- [16] G.R. Stewart, Z. Fisk, J.O. Willis and J.L. Smith, *Phys. Rev. Lett.* 52 (1984) 679.

- [17] W. Schlabit, J. Baumann, B. Pollit, U. Rauschwalbe, H.M. Mayer, U. Ahlheim and C.D. Bredl, *Z. Phys. B* 62 (1986) 171.  
T.T.M. Palstra, A.A. Menovsky, J. van den Berg, A.J. Dirkmaat, J.G. Niewenhuys and J.A. Mydosh, *Phys. Rev. Lett.* 55 (1985) 2727.  
M.B. Maple, J.W. Chen, Y. Dalichaouch, Y. Kohara, C. Rossel, M.S. Torikachivili, H.W. McElfresh and J.D. Thompson, *Phys. Rev. Lett.* 56 (1986) 185.
- [18] V. Müller, C. Roth, D. Maurer, E.W. Scheidt, K. Lüders, E. Bucher and H.E. Bömmel, *Phys. Rev. Lett.* 58 (1987) 1224.  
R.A. Fisher, S. Kim, B.F. Woodfield, N.E. Phillips, L. Taillefer, K. Hasselbach, J. Flouquet, A.L. Giorgi and J.L. Smith, *Phys. Rev. Lett.* 62 (1989) 1411.  
K. Hasselbach, L. Taillefer and J. Flouquet, preprint (1989).
- [19] G. Aeppli, E. Bucher, A.I. Goldman, G. Shirane, C. Broholm and J.K. Kjems, *J. Magn. Magn. Mat.* 76 & 77 (1988) 385.
- [20] J.P. Brison, A. Ravex, J. Flouquet, Z. Fisk and J.L. Smith, *J. Magn. Magn. Mat.* 76 & 77 (1988) 525.
- [21] Y.J. Uemura, W.J. Kossler, X.H. Yu, H.E. Shone, J.R. Kempton, C.E. Stronach, S. Barth, F.N. Gygax, B. Hitti, A. Schenck, C. Baines, W.F. Lankford, Y. Onuki and T. Komatsubara, *Phys. Rev. B* 39 (1989) 4726.
- [22] H. Nakamura, Y. Kitaoka, H. Yamada and K. Asayama, *J. Magn. Magn. Mat.* 76 & 77 (1988) 517.
- [23] U. Rauchschwalbe, F. Steglich, A. de Visser and J.J.M. Franse, *J. Magn. Magn. Mat.* 63 & 64 (1987) 347.
- [24] U. Rauchschwalbe, W. Lieke, C.D. Bredl, F. Steglich, J. Aarts, K.M. Martini and A.C. Mota, *Phys. Rev. Lett.* 49 (1982) 1448.
- [25] F. Steglich, *J. Phys. Chem. Solids* 50 (1989) 225.
- [26] U. Ahlheim, M. Winkelmann, C. Schank, C. Geibel, F. Steglich and A.L. Giorgi, *Physica B* 163 (1990) 393.
- [27] B. Batlogg, D.J. Bishop, E. Bucher, B. Golding, Jr., A.P. Ramirez, Z. Fisk, J.L. Smith and H.R. Ott, *J. Magn. Magn. Mat.* 63 & 64 (1987) 441.
- [28] B. Lloret, B. Chevalier, B. Buffat, J. Etourneau, S. Quezel, A. Lamharrar, J. Rossat-Mignod, R. Calemczuk and E. Bonjour, *J. Magn. Magn. Mat.* 63 & 64 (1987) 85.
- [29] F. Steglich, G. Sparn, R. Moog, S. Horn, A. Grauel, M. Lang, M. Nowak, A. Loidl, A. Krimmel, K. Knorr, A.P. Murani and M. Tachiki, *Physica B* 163 (1990) 19.
- [30] C. Geibel, U. Ahlheim, A.L. Giorgi, G. Sparn, H. Spille, F. Steglich and W. Suski, *Physica B* 163 (1990) 194.
- [31] H. Spille, U. Rauchschwalbe and F. Steglich, *Helv. Phys. Acta* 56 (1983) 165.
- [32] J.L. Smith, Z. Fisk, J.O. Willis, B. Batlogg and H.R. Ott, *J. Appl. Phys.* 55 (1984) 1996.
- [33] F. Steglich, U. Ahlheim, U. Rauchschwalbe and H. Spille, *Physica B* 148 (1987) 6.  
U. Ahlheim, P. van Aken, H. Spille and F. Steglich, *Helv. Phys. Acta* 61 (1988) 518.
- [34] See, e.g., F. Steglich, *Z. Phys. B* 23 (1976) 331.
- [35] U. Ahlheim, M. Winkelmann, P. van Aken, C.D. Bredl, F. Steglich and G.R. Stewart, *J. Magn. Magn. Mat.* 76 & 77 (1988) 520.
- [36] C.D. Bredl, S. Horn, F. Steglich, B. Lüthi and R.M. Martin, *Phys. Rev. Lett.* 52 (1984) 1982.
- [37] H.R. Ott, H. Rudigier, Z. Fisk and J.L. Smith, *Phys. Rev. B* 31 (1985) 1651.
- [38] U. Rauchschwalbe, C.D. Bredl, F. Steglich, K. Maki and P. Fulde, *Europhys. Lett.* 3 (1987) 757.
- [39] G. Knopp, A. Loidl, K. Knorr, L. Pawlak, M. Duczmal, R. Caspary, U. Gottwick, H. Spille, F. Steglich and A.P. Murani, *Z. Phys. B* 77 (1989) 95.
- [40] F.R. de Boer, J.C.P. Klaasse, P.A. Veenhuizen, A. Böhm, C.D. Bredl, U. Gottwick, H.M. Mayer, L. Pawlak, U. Rauchschwalbe, H. Spille and F. Steglich, *J. Magn. Magn. Mat.* 63 & 64 (1987) 91.
- [41] G. Knopp, A. Loidl, R. Caspary, U. Gottwick, C.D. Bredl, H. Spille, F. Steglich and A.P. Murani, *J. Magn. Magn. Mat.* 74 (1988) 341.
- [42] G. Sparn, R. Caspary, U. Gottwick, A. Grauel, U. Habel, M. Lang, M. Nowak, R. Scheffzyk, W. Schiebeling, H. Spille, M. Winkelmann, A. Zuber, F. Steglich and A. Loidl, *J. Magn. Magn. Mat.* 76 & 77 (1988) 153.
- [43] D.L. Cox and N. Grewe, *Z. Phys. B* 71 (1988) 321.
- [44] N. Grewe and B. Welslau, *Solid State Commun.* 65 (1988) 437.
- [45] A. Böhm, R. Caspary, U. Habel, L. Pawlak, A. Zuber, F. Steglich and A. Loidl, *J. Magn. Magn. Mat.* 76 & 77 (1988) 150.
- [46] Z. Blazina and Z. Ban, *Z. Naturforsch.* 28b (1973) 561.
- [47] U. Rauchschwalbe, U. Gottwick, U. Ahlheim, H.M. Mayer and F. Steglich, *J. Less-Common Metals* 11 (1985) 265.
- [48] G. Cordier, E. Czech, H. Schäfer and P. Woll, *J. Less-Common Metals* 110 (1985) 327.
- [49] A. Baran, W. Suski, O.J. Zogal and T. Mydlay, *J. Less-Common Metals* 121 (1986) 175.
- [50] M. Drules, A. Baran, B. Stalinski, W. Suski, R. Felten, F. Steglich and L. Pawlak, *Thermochimica Acta* 139 (1989) 219.
- [51] R. Moog and G. Sparn, unpublished results.